Dalton Transactions

Accepted Manuscript

This is an *Accepted Manuscript*, which has been through the RSC Publishing peer review process and has been accepted for publication.

Accepted Manuscripts are published online shortly after acceptance, which is prior to technical editing, formatting and proof reading. This free service from RSC Publishing allows authors to make their results available to the community, in citable form, before publication of the edited article. This *Accepted Manuscript* will be replaced by the edited and formatted *Advance Article* as soon as this is available.

To cite this manuscript please use its permanent Digital Object Identifier (DOI®), which is identical for all formats of publication.

More information about *Accepted Manuscripts* can be found in the **Information for Authors**.

Please note that technical editing may introduce minor changes to the text and/or graphics contained in the manuscript submitted by the author(s) which may alter content, and that the standard **Terms & Conditions** and the **ethical guidelines** that apply to the journal are still applicable. In no event shall the RSC be held responsible for any errors or omissions in these *Accepted Manuscript* manuscripts or any consequences arising from the use of any information contained in them.

Table of Contents

Metal-organic framework MIL-88A displays active MB dye degradation performance.

TOC Figure

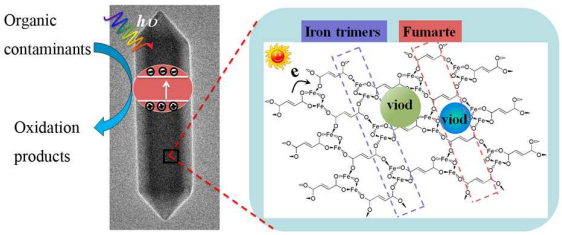

Cite this: DOI: 10.1039/c0xx00000x

www.rsc.org/xxxxxx

ARTICLE TYPE

Metal-organic frameworks MIL-88A hexagonal microrods as a new photocatalyst for efficient decolorization of methylene blue dye

Wen-Tao Xu,[a] Lin Ma,[a] Fei Ke,[b] Fu-Min Peng,[a] Geng-Sheng Xu,[a] Yu-Hua Shen,[a] Jun-Fa Zhu,[b] Ling-Guang Qiu,[a] Yu-Peng Yuan*[a]

Received (in XXX, XXX) Xth XXXXXXXXX 20XX, Accepted Xth XXXXXXXXX 20XX
DOI: 10.1039/b000000x

Metal-organic frameworks (MOFs) MIL-88A hexagonal mocrorods as a new photocatalyst show active performance for methylene blue (MB) dye decolorization using visible light. MB decolorization over MIL-88A photocatalyst follows the first-order kinetics. The addition of H_2O_2 electron acceptor can markedly enhance the photocatalytic MB decoloration performance of MIL-88A. Moreover, MIL-88A showed very stable activity for MB decoloration after four consecutive usages. Owing to the advantages of visible light response, low cost and abundance in nature, this active MIL-88A MOFs photocatalyst would have great potential for environmental purification.

Introduction

Photocatalytic reactions, including water splitting, organic pollutants degradation, and CO_2 reduction into valuable energy-rich fuels have attracted a great deal of interests.[1, 2] In the past several decades, it has attracted tremendous attentions on exploring new photocatalysts to solve environmental issues.[3-8] Since the first demonstration of UV light-driven organic pollutants degradation with semiconducting TiO_2, several UV-active and visible-response photocatalysts, such as ZnO, WO_3, CdS, ZnS have been demonstrated as active photocatalysts for photodegradation of organic pollutants in gas and aqueous phase, but their limitations in terms of the requirements of UV excitation and photo-corrosion have also been verified.[9-16] Among these photocatalysts, TiO_2 has received tremendous attention owing to the advantages of high photocatalytic activity, low-cost, non-toxicity, excellent chemical stability, and abundance in nature.[17-20] Recently, carbon based materials, such as C60, carbon nanotubes, and grapheme, have also been widely reported as visible-light-response photocatalysts because of their stability and abundance in nature.[21-25] Presently, it still remains a great challenge to develop a photocatalyst that can work for pollutants degradation with high efficiency, acceptable stability and low cost when irradiating by visible light.

Metal-organic frameworks (MOFs) are a class of crystalline materials that are constructed by polyfunctional molecular building blocks and metal or metal clusters connecting nodes. Owing to their elegant topology and high surface area, MOFs have attracted intensive attentions in gas storage, molecular sensing, separation, and catalysis.[26-28] Recently, photoactive MOFs behaving as semiconductors have been used to eliminate the contamination of organic pollutants.[29-34] Comparing with reported photocatalysts, such as TiO_2 and ZnO, photoactive MOFs have following advantages: 1) the intrinsic porosity can facilitate the diffusion of the organic pollutants and products through the open channels, which is very essential for high photocatalytic reaction efficiency; 2) the modular nature of MOFs synthesis allows the rational design and fine tuning of these new class of photocatalysts at the molecular level, making the electronic structure of MOFs photocatalysts -easily tuned; 3) versatile synthetic strategies, including solvothermal, vapor diffusion, emulsion-assistant precipitation, and ultrasonication, allow a high degree of crystalline quality and morphologies of MOFs photocatalysts.[29] In 2007, Garcia *et al* firstly demonstrated that $Zn_4O(BDC)_6$ MOF (MOF-5) displayed photocatalytic activity for phenol degradation comparable to that of P25 TiO_2.[30] Natarajan *et al* used Co, Ni, and Zn - MOFs to degrade the rhodamine B, orange G, Remazol Brilliant Blue R, and methylene blue dyes.[31] Gascon *et al* studied the gas-phase propene oxidation over isoreticular MOFs of IRMOF-1, IRMOF-2, IRMOF-7, IRMOF-8, and IRMOF-9, and they found that IRMOF-8 displayed higher activity than that of ZnO.[32] Recently, Wang *et al* reported that Zn and Cd MOFs displayed active MB degradation performance under UV-light irradition.[33] Etaiw *et al* used organotin-polymer $[(Me_3Sn)_4Fe(CN)_6]$ for MB decolorization.[34] Although these very impressive results showed that MOFs could be attractive photocatalysts for solving environmental issues, the photocatalytic properties of MOFs have remained in their infancy state.

Herein, we report a new MOFs photocatalyst of MIL-88A for MB degradation. MIL-88A is a 3D framework built-up from trimers of iron (III) octahedral linked to fumarte dianions and exhibits cages together with open channels running along the c axis.[35] In comparison with the reported MOFs photocatalysts, MIL-88A possesses a very large volume swelling upon exposing to polar solvent. For example, hydrated MIL-88A exhibits a large and reversible swelling (almost doubling (85 %) of its cell volume) while fully maintaining its open-framework topology.[36]

It is well known that photocatalytic reaction is a surface reaction in which the reactants need to be pre-adsorbed on the surface of a photocatalyst, following the redox reactions and desorption of the reaction products. Therefore, this large swelling effect in MIL-88A is very favorable for mass transport in photocatalytic reactions. In other words, the reactants can be easily adsorbed onto the reaction sites through this large volume swelling. Presently, there is no concerns on the photocatalytic performance of MIL-88A for organic pollutants degradation. Herein, we reported the active photocatalytic performance of MIL-88A for MB dye degradation using visible light. The addition of H_2O_2 electron acceptor can greatly enhance the photocatalytic MB degradation of MIL-88A. Moreover, the MIL-88A photocatalyst possesses high stability in aqueous solution. No evident activity loss was observed after four consecutive cycles for MB degradation.

Materials and methods

Reagents and chemicals

All reagents were analytical grade and used without further purification unless noted. Iron (III) chloride hexahydrate (99%), fumaric acid (HO_2C-C_2H_2-CO_2H; 99%), and hydrogen peroxide (30%) were purchased from Aladdin Chemical Reagent Co. Ltd, China. Ultrapure water from a Milipore Milli-Q system was used to prepare aqueous solutions for MIL-88A synthesis and for the degradation experiments.

Synthesis of MIL-88A photocatalyst

MIL-88A photocatalyst was prepared according to the previous synthesis protocol with some modifications in solution concentration and reaction time.[37] Typically, 5 mmol $FeCl_3 \cdot 6H_2O$ and 5 mmol fumaric acid were first dissolved in 25 mL ultrapure water, and then the homogeneous solution was transferred into a 60 mL Teflon-lined stainless steel autoclave and heated to 65 ^oC for 12 h. After cooling to room temperature, the product was washed with water and ethanol repeatedly, and then dried in a vacuum oven after centrifugation.

Photocatalysts characterization

X-ray powder diffraction (XRD) patterns of the obtained MIL-88A samples were carried out on a DX-2700 X-ray diffractometer (Haoyuan, China) using Cu Kα1 radiation at a scan rate of 1 °/min. The acceleration voltage and the applied current were 40 kV and 40 mA, respectively. The morphologies and size of the MIL-88A samples were observed by field emission scanning electron microscopy (SEM: JEOL JSM-7600F) and transmission electron microscopy (TEM: JEOL JEM-2100F). TEM was operated at an accelerating voltage of 200 kV. UV–vis diffuse reflectance spectra (DRS) were measured over the spectral range 320-800 nm on a Lambda 750 UV/Vis/NIR spectrophotometer (Perkin Elmer, USA). $BaSO_4$ was used as a reflectance standard. X-ray photoelectron spectra (XPS) of the as-prepared MIL-88A were recorded on an ESCALAB250 spectrometer (Thermo-VG Scientific) using Mg $K\alpha$ radiation (1253.6 eV) and the binding energy values were calibrated with respect to C (1s) peak (284.6 eV).

Photocatalytic degradation of MB

The model reaction, MB dye degradation through photon oxidation, was used for evaluating the photocatalytic activity of the MIL-88A hexagonal microrods using visible light at room temperature. The distance between the light source and the beaker containing MIL-88A and MB solution was fixed at 10 cm. MIL-88A photocatalyst (40 mg) was dispersed into 100 mL MB aqueous solution (1×10^{-4} mol • L^{-1}) in a 250 ml beaker. The pH value of the suspension was adjusted to neutral (pH=7.0). The suspension was first magnetically stirred in dark for 30 min to establish the adsorption-desorption equilibrium (see Fig. S1, MB concentration keeps constant after 10 min adsorption over MIL-88A), then irradiated by a 300 W Xenon lamp to trigger the photocatalytic reaction (light inensity ~ 800 mW/cm^2). A 420 nm cut-off filter was used to provide the visible light. The MB solution was withdrawn periodically and centrifuged to separate MIL-88A photocatalyst for analysis. The MB concentration change was monitored by measuring the absorption at λ=664 nm using a UV-visible spectrophotometer (UV-1800, Shimadzu). The average values of three experimental results were used to draw the plot.

Results and discussion

Sample characterizations

The X-ray powder pattern of obtained products shows that the as-prepared products are crystalline solid, as shown in Fig.1. Férey *et al* found that the MIL-88A shows an unusual flexibility upon adsorption of polar solvent molecules.[36] We found that the as-prepared samples are well matched with the hydrated MIL-88A sample, $Fe^{III}_3O(H_2O)_3\{^-O_2C$-$C_2H_2$-$CO_2^-\}_3\cdot\{^-O_2C$-$CH_3\}\cdot nH_2O$, wherein a large number of free water molecules are existing in the channels and cages of the MIL-88A.[36] The existing of the H_2O molecules within the MIL-88 frame should be caused by the low drying temperature of 60 ^oC, while the these water molecules should be removed over 150 ^oC. XRD analysis clearly revealed that the obtained products are single phase MIL-88A MOFs. The average crystallite size of the obtained MIL-88A is ~ 24.7 nm calculated by Scherrer equation using three strongest lines (corresponding to (010), (011), and (002) diffraction plane). The UV-vis spectrum (Fig. 2) of the MIL-88A sample shows several distinct absorption peaks and the absorption edge is around ~ 650 nm, which should be caused by the optical transitions of ligand-to-metal charge transfer (LMCT). The band gap energy (E_g) is estimated to be 2.05 eV by Tauc plot (see the inset in Fig. 2), which is consistent with the colour of the MIL-88A (see inset of Fig. 2). We also measured the N_2 adsorption-desorption isotherm of the obtained MIL-88A. However, we cannot obtain the true physical parameters, including the surface area, pore size and pore volume because the MIL-88A flexible structures are all in a closed pore configuration after degassing and not accessible to N_2 adsorption (see Fig. S2).[38]

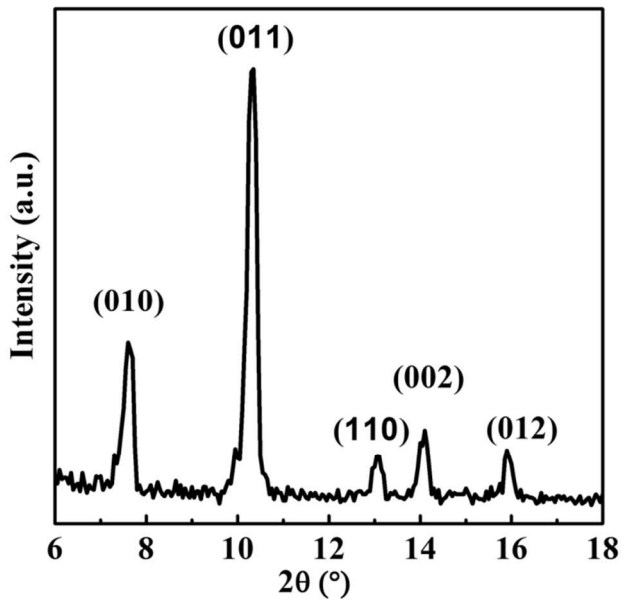

Fig.1 XRD pattern of the obtained MIL-88A product.

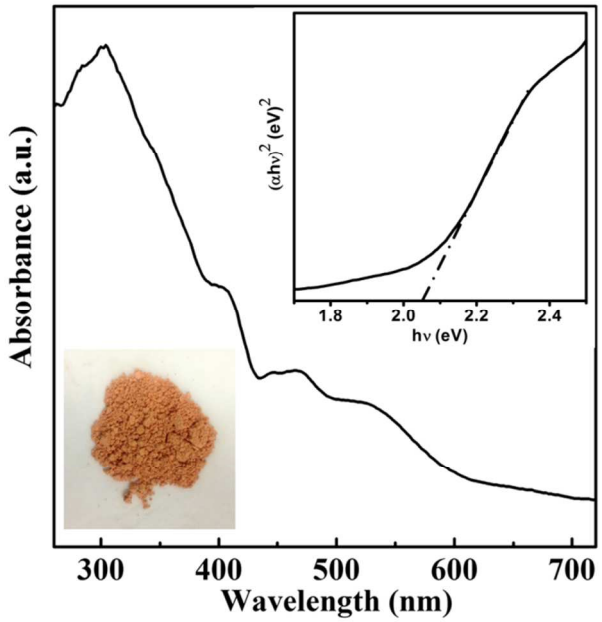

Fig.2 UV-visible absorption spectra of MIL-88A photocatalyst. The inset shows the color of obtained MIL-88A.

SEM observation reveals that the as-prepared MIL-88A photocatalysts are well-crystallized hexagonal microrods of over 2 μm in length and less than 500 nm in diameter (Fig. 3a). Importantly, the size distribution of these MIL-88A rods is relatively uniform with few exceptions. Further observation by TEM (Fig. 3b) also shows a uniform size distribution and morphology of the crystalline MIL-88A particles. Each hexagonal microrod is ~ 2.6 μm in length and ~ 500 nm in width. Combined with the XRD result, SEM and TEM observations indicate that the prepared MIL-88A is polycrystalline. The hexagonal structure can be further revealed by the magnified image (Fig. 3c). However, the SAED and high-resolution TEM images of the MIL-88A are not attainable because these MIL-88A microrods tend to be destroyed under high energy focusing electron beam bombing (Fig. 3d). Therefore we cannot determine the exact growth direction and crystallographic facets of MIL-88A hexagonal microrods.

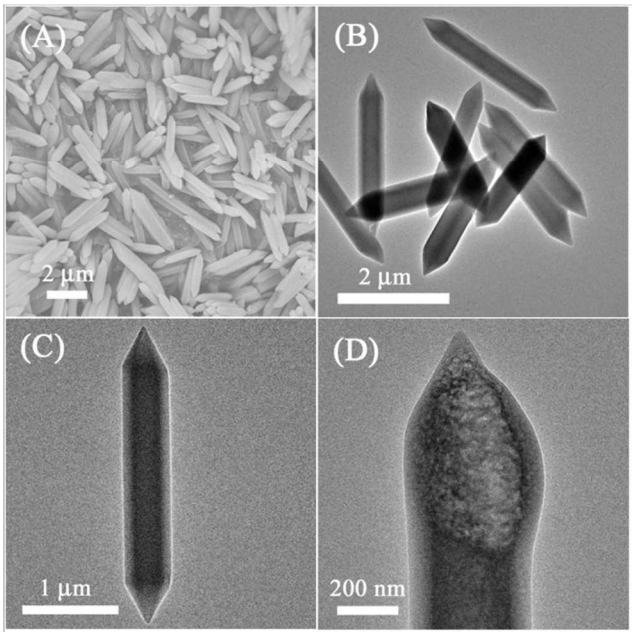

Fig. 3 (A) SEM image and TEM micrographs of (B) typical TEM image; (C); magnified image; (D) destroyed image of MIL-88A.

Photocatalytic activities

The photocatalytic MB degradation was conducted as the model reaction to investigate the performance of the MIL-88A photocatalyst. The MIL-88A concentration was fixed at 0.4 g • L^{-1} in all experiments. The photocatalytic activity of MIL-88A photocatalyst was monitored in terms of the MB color change by measuring its maximum absorbance at λ_{max}=664 nm. The photocatalytic performance of commercial P25 TiO_2 under visible light irradiation was also measured under the same experimental conditions for comparison. Control experiments show that no MB degradation was observed over MIL-88A photocatalyst and H_2O_2 without the light irradiation (Fig. 4f). In contrast, ~ 5% MB was self-discolored after 20 min visible light irradiation (Fig. 4a), while ~ 16% MB was degraded when using MIL-88A photocatalyst for 20 min visible light irradiation (Fig. 4c). Thus, it can be concluded that MIL-88A shows the photocatalytic activity for MB discoloration, although the photodegradation rate is low. Notably, MIL-88A shows a 2 times higher MB discoloration than P25 TiO_2 under the same condition. Only ~ 7% MB was degraded over P25 TiO_2 after 20 min visible light irradiation (Fig. 4b), while ~ 16% MB was degraded over MIL-88A. The reaction mechanism for MB decoloration could be discussed based on semiconductor theory. Electrons (e^-) will be excited from the valence band (VB) to the conduction (CB) band when MIL-88A was illuminated by photons with energy equal to or greater than its band gap, leaving hole (h^+) in valence band (equation 1). The photoexcited holes have strong oxidant ability and can directly oxidize adsorbed organic molecules or react with

hydroxyl ion (OH^-) to generate hydroxyl radical (•OH) (equation 2), as confirmed by VB XPS spectrum (Fig. S3). The VB edge of MIL-88A locates at ~ 2.3 eV, indicating that the photoexcited holes possess strong oxidation capacity for organic pollutants degradation. The formed •OH possesses strong oxidation capacity and can also oxidize the surface adsorbed organic molecules. Meanwhile, photoexcited electrons can be trapped by molecular oxygen to form superoxide radical (O_2^-) (equation 3), which also possesses strong oxidant ability to decolorize the MB molecules， as shown in Schem 1.

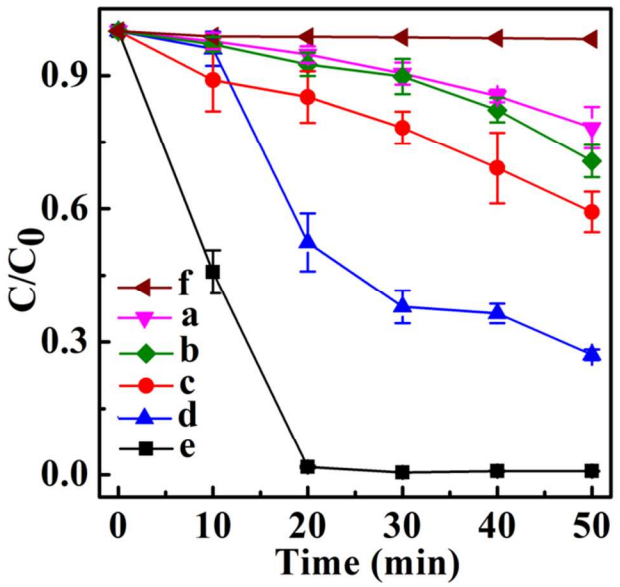

Fig.4 MB decolorization profile with visible light irradiation ondifferent conditions, (a) MB self-decolorization; (b) using P25 TiO_2 as photocatalyst; (c) using MIL-88A as photocatalyst; (d) only addition of H_2O_2 electron acceptor; (e) using MIL-88A photocatalyst and H_2O_2 electron acceptor; and (f) using MIL-88A photocatalyst and H_2O_2 without light irradiation.

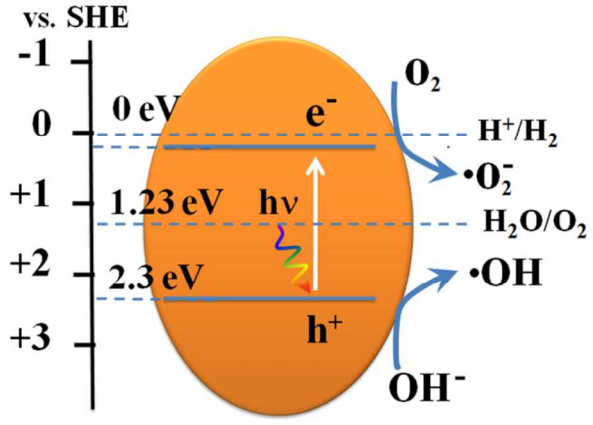

Scheme 1 Schematic illustration of the energy position of the MIL-88A.

$$MIL - 88A + h\nu \rightarrow h^+ + e^- \quad (1)$$

$$h^+ + OH^- \rightarrow \cdot OH \quad (2)$$

$$e^- + O_2 \rightarrow \cdot O_2^- \quad (3)$$

$$H_2O_2 + e^- \rightarrow \cdot OH + OH^- \quad (4)$$

The MB photodegradation over MIL-88A follows the first-order kinetics model (Fig. 5). The first-order kinetics can be written as $\ln(C_0/C)=Kt$ (Langmuir–Hinshelwood model), wherein C_0 is the initial MB concentration, C is the *t* time's MB concentration, *t* is the reaction time, and K is the kinetic rate constant. The values of K can be calculated from the slope and the intercept of the he linear plot. The rate constants for MB self-degradation and photodegradation over MIL-88A are 0.004 and 0.010 min^{-1} under visible light irradiation, respectively (Fig. 5a and 5b). The present finding demonstrates that the MIL-88A hexagonal microrods are a visible-light-response photocatalyst for removal of MB pollutant.

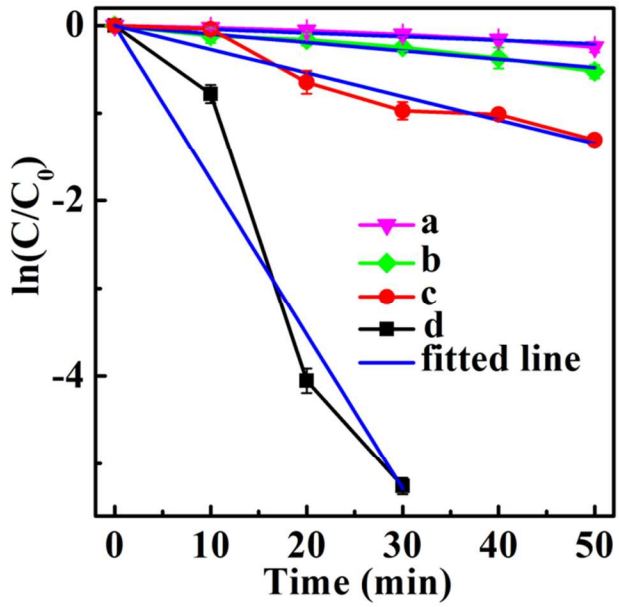

Fig.5 Reaction kinetics of MB over MIL-88A photocatalyst under visible light irradiation on different conditions, (a) MB self-decolorization; (b) using MIL-88A as photocatalyst; (c) only addition of H_2O_2 electron acceptor; and (d) using MIL-88A photocatalyst and H_2O_2 electron acceptor.

The photocatalytic activity of MIL-88A for MB decolorization can be greatly enhanced by the addition of hydrogen peroxide (H_2O_2) electrons acceptor. As stated above, the photocatalytic reaction starts from the generation of electron-hole pairs. The photoexcited holes either react with organic molecules directly or react with OH^- to generate •OH for further oxidation reaction. The electron-hole recombination always reduces the photocatalytic reaction efficiency. Therefore, the introduction of external electron acceptor is expected to suppress the electron-hole recombination and enhance the photocatalytic efficiency. enhanced photodegradation efficiency with the addition of H2O2 as an electron accepto can be explained by equation 4.[39] The addition of H_2O_2 ($4x10^{-3}$ $mol{\cdot}L^{-1}$) can markedly enhance the MB decolorization rate over MIL-88A, while the addition of H_2O_2 without light irradiation does not enhance the MB degradation rate over MIL-88A, as shown in Fig.4f. 20 min visible light irradiation induces the MB total degradation (Fig. 4e), whereas only less than 50% MB was degraded when only H_2O_2 was used in the reaction (*K* is 0.027) (Fig. 4d). Considering the consumption of H_2O_2 during the MB photocatalytic degradation, the MB photodegradation over MIL-88A in the presence of H_2O_2 can be treated as pseudo-first order reaction kinetics. The rate

constant is 0.176 min^{-1} in present reaction, which is over 17 times higher than that in the absence of H_2O_2. Synergy index (*SI*), defined as $SI=K_{(H2O2+MIL-88A)}/(K_{H2O2}+K_{MIL-88A})$, is 4.7, indicating a pronounced synergic effect with the electron acceptor addition. The enhanced photocatalytic MB degradation rate with H_2O_2 addition should be attributed to the scavenger of the excited electrons from MIL-88A by H_2O_2, leading to efficient suppression of the electron-hole recombination. The remained active holes on MIL-88A could oxidize OH^- to generate •OH radicals in the solution. It is well known that •OH radicals can efficiently react with terephthalic acid (TA) in basic solution to form 2-hydroxy-terephthalic acid (TAOH). The TAOH can emit strong fluorescence signal at 426 nm.[40, 41] Therefore, the intensity of TAOH fluorescence signal can qualitatively identify the amount of the formed •OH radicals. We have used this reaction to compare the amount of the formed •OH radicals under various reaction conditions in order to verify the enhanced holes' amount by H_2O_2 addition (Fig. 6). Control experiments confirm that there is no TAOH fluorescence peak without MIL-88A photocatalysts using visible light illumination (Fig. 6a), while a relative weak TAOH fluorescent peak were observed upon only MIL-88A photocatalyst or H_2O_2 using visible light (Fig. 6b and Fig. 6c). This result further confirms that the excitation of electron-hole pairs was occurred in MIL-88A upon visible light irradiation. As expected, the H_2O_2 addition induces a remarkably increased fluorescence intensity of TAOH in comparison to the pristine MIL-88A photocatalyst (Fig. 6d). Moreover, the fluorescence intensity algebraic addition of only MIL-88A and only H_2O_2 system is still obviously lower than that of the system with MIL-88A and H_2O_2. This result confirms that the addition of H_2O_2 electron acceptor suppresses charge recombination so that the photogenerated holes can generate more •OH radicals towards high TAOH concentration and stronger fluorescence signal, thus enhancing the photocatalytic MB degradation rate.

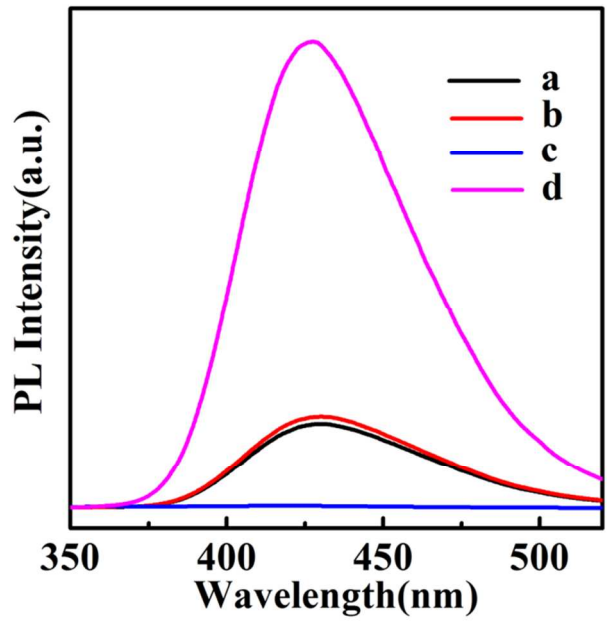

Fig.6 Photoluminescence spectra of TAOH formed by the reaction of TA with ·OH radicals generated from different samples under visible light irradiation for 10 min, (a) in the presence of H_2O_2 only; (b) over MIL-88A photocatalyst; (c) without photocatalyst and H_2O_2; and (d) over MIL-88A photocatalyst with H_2O_2 electron acceptor.

The long-term stability of the present MIL-88A photocatalyst was also examined. After each run of the MB total decolorization, the MIL-88A was centrifuged and re-dispersed into the following MB solution. To maintain a constant concentration of the MIL-88A, the same amount of MB was used for each experiment. Fig. 7 shows the time course of MB decolorization during four consecutive cycles. No obvious activity loss for MB decolorization was observed during these four consecutive reactions, indicating the excellent stability of MIL-88A as a photocatalyst.

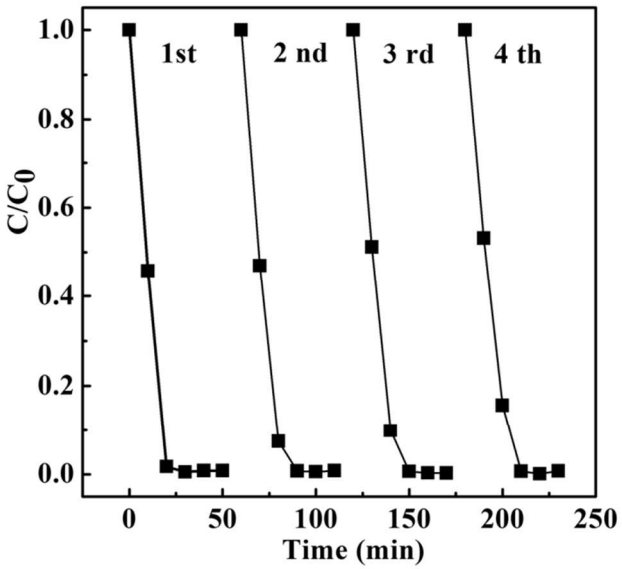

Fig.7 Photocatalytic MB decolorization during four consecutive runs over MIL-88A photocatalyst with H_2O_2 electron acceptor.

The crystal structure and chemical states of MIL-88A before and after 4 cycle reactions were further examined by XRD and XPS analysis, as shown in Fig.8. The identical XRD pattern before and after usage demonstrates that no structural transformation was occurred in the repeated photocatalytic reactions (see Fig. 8A). Fig.8B shows the Fe 2p binding energy spectra before and after repeated usages. The binding energy of 711.8 and 725.6 eV can be ascribed to Fe $2p_{3/2}$ and Fe $2p_{1/2}$, respectively. The peak separation, namely, $\Delta=2p_{1/2}-2p_{3/2}=13.8$ eV, is very similar to those reported for Fe_2O_3, indicating that the two peaks belong to Fe^{3+} of MIL-53(Fe).[42] The XPS data did not change after 4 cycle usages, further indicating the long-term stability of MIL-88A as a photocatalyst. Moreover, inductively coupled plasma atomic emission spectrometer (ICP-AES; M6, Thermo Elemental, USA) analysis reveals that only trace amount of Fe ions was detected in the centrifuged solution after 4 cycle usages.

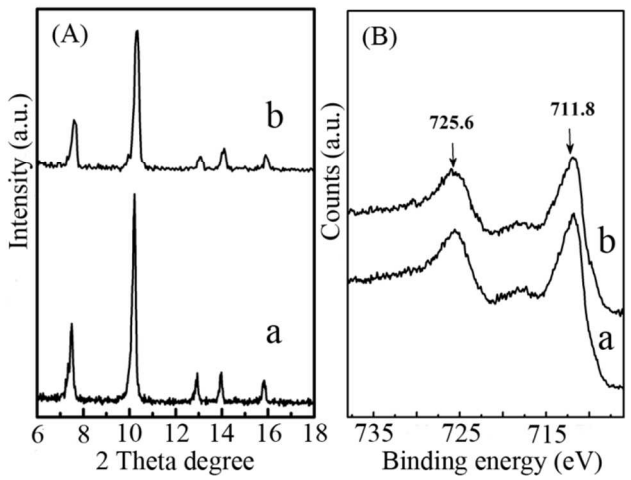

Fig.8 XRD patterns and XPS spectra of MIL-88A photocatalyst (a) before and (b) after four consecutive runs for MB decolorization.

Conclusions

MIL-88A hexagonal microrods were demonstrated as a new MOFs photocatalyst for MB photodegradation using visible light. The MB degradation reaction over MIL-88A follows the first-order kinetics with a rate constant of 0.01 min^{-1}. And the addition of H_2O_2 electron acceptor can markedly enhance the MB degradation efficiency. Importantly, MIL-88A displays high chemical stability for repeated MB degradation reactions. This work provides new insights on developing MOFs photocatalysts and further demonstrates the great potential of MOFs to be active photocatalysts for environmental purification.

Acknowledgements

This work was supported by the National Natural Science Foundation of China (51002001), the "Hundred Talents Program" of the Chinese Academy of Sciences, and the State "211 Project" of Anhui University, China.

Notes and references

[a] *Laboratory of Advanced Porous Materials and School of Chemistry and Chemical Engineering, Anhui University, Hefei 230039, China. Fax: +86 551 65108212; Tel: +86 551 65108212; E-mail: yupengyuan@ahu.edu.cn*

[b] *National Synchrocyclotron Radiation Laboratory, University of Science and Technology of China, Hefei 230029, China*

1 W. J. Ong, M. M. Gui, S. P. Chai and A. R. Mohamed, *RSC Adv.*, 2013, **3**, 4505.
2 X. Wu, S. Yin, Q. Dong, C. Guo, H. Li, T. Kimura and T. Sato, *Appl. Catal. B: Environ*., 2013, **142-143**, 450.
3 X. B. Chen, S. H. Shen, L. J. Guo and S. S. Mao, *Chem. Rev*., 2010, **110**, 6503.
4 H. Tong, S. X. Ouyang, Y. P. Bi, N. Umezawa, M. Oshikiri and J. H. Ye, *Adv. Mater*., 2011, **24**, 229.
5 A. Kudo and Y. Miseki, *Chem. Soc. Rev*., 2009, **38**, 253.
6 F. E. Osterloh, *Chem. Mater*. 2007, **20**, 35.
7 Y. P. Yuan, S. W. Cao, Y. S. Liao, L. S. Yin and C. Xue, *Appl. Catal. B: Environ*., 2013, **140-141**,164.
8 T. B Li, G. Chen, C. Zhou, Z. Y. Shen, R. C. Jin and J. X. Sun, *Dalton Trans*., 2011, **40**, 6751.
9 N. F. Steven and A. J. Bard, *J. Am. Chem. Soc*., 1977, **99**, 303.
10 M. R. Hoffmann, S. T. Martin, W. Choi and D. W. Bahnemann, *Chem. Rev*., 1995, **95**, 69.
11 C. S. Li, D. Q. Zhang and J. C. Yu, *Environ. Sci Technol*., 2009, **43** 7079.
12 A. Mills and S. L. Hunte, *J. Photochem. Photobio A: Chem*., 1997, **108**, 1.
13 C. W. Raubach, Y. B. B. D. Santana, M. M. Ferrer, P. G. C. Buzolin, J. R. Sambrano and E. Longo, *Dalton Trans*. 2013, **42**, 11111.
14 J. X. Sun, Y. P. Yuan, L. G. Qiu, X. Jiang, A. J. Xie, Y. H. Shen and J. F. Zhu, *Dalton Trans*. 2012, **41**, 6756.
15 M. D. Hernandez-Alonso, F. Fresno, S. Suarez and J. M. Coronado, *Energy Environ. Sci*., 2009, **2**, 1231.
16 S. J. Yang, J. H. Im, T. Kim, K. Lee and C. R. Park, *J. Hazard. Mater*., 2011, **186**, 376.
17 Y. J. Wang, Q. S. Wang, X. Y. Zhan, F. M. Wang, M. Safdar and J. He, *Nanoscale*, 2013, **5**, 8326.
18 X. Y. Pan, M. Q. Yang, X. Z. Fu, N. Zhang and Y. J. Xu, *Nanoscale*, 2013, **5**, 3601.
19 W. J. Ong, L. L. Tan, S. P. Chai, S. T. Yong and A. R. Mohamed, *Nanoscale*, 2013, DOI: 10.1039/C3NR04655A.
20 M. A. Lazar and W. A. Daoud, *RSC Adv*., 2013, **3**, 4130-4140.
21 G. Lui, J. Y. Liao, A. Duan, Z. S. Zhang, M. Fowler and A. P. Yu, *J. Mater. Chem. A*, 2013, **1**, 12255.
22 J. Yu, T. Ma, G. Liu and B. Cheng, *Dalton Trans*., 2011, **40**, 6635.
23 W. J. Ong, M. M. Gui, S. P. Chai and A. R. Mohamed, *RSC Adv*., 2013, **3**, 4505.
24 Y. H. Hu, H. Wang, B. Hu, *ChemSusChem*., 2010, **3**, 782.
25 Q. J. Xiang, J. G. Yu and M. Jaroniec, *Nanoscale*, 2011, **3**, 3670.
26 L. J. Murray, M. Dinca and J. R. Long, *Chem. Soc. Rev*., 2009, **38**, 1294.
27 J. Y. Lee, O. K. Farha, J. Roberts, K. A. Scheidt, S. T. Nguyen and J. T. Hupp, *Chem. Soc. Rev*., 2009, **38**, 1450.
28 J. R. Li, R. J. Kuppler and H. C. Zhou, *Chem. Soc. Rev*., 2009, **38**, 1477.
29 J. L. Wang, C. Wang and W. B. Lin, *ACS Catal*., 2012, **2**, 2630.
30 X. L. X. Francesc, A. Corma and H. Garcia, *J. Phys. Chem. C*., 2007, **111**, 80.
31 P. Mahata, G. Madras and S. Natarajan, *J. Phys. Chem. B*., 2006, **110**, 137598.
32 J. Gascon, M. D. Hernández-Alonso, A. R. Almeida, G. P. M. van Klink, F. Kapteijn and G. Mul, *ChemSusChem*., 2008, **1**, 981.
33 X. Wang, J. Huang, L. Liu, G. Liu, H. Lin, J. Zhang, N. Chen and Y. Qu, *CrystEngComm*, 2013, **15**, 1960.
34 S. E. H. Etaiw, M. M. El-bendary, *Appl. Catal. B: Environ*., 2012, **126**, 326.
35 C. Serre, F. Millange, S. Surble and G. Ferry, *Angew. Chem. Int. Ed*., 2004, **43**, 6286.
36 C. Mellot-Draznieks, C. Serre, S. Surble, N. Audebrand and G. Fery, *J. Am. Chem. Soc*., 2005, **127**, 16273.
37 P. Horcajada1, T. Chalati, C. Serre, B. Gillet, C. Sebrie, T. Baati, J. F. Eubank, D. Heurtaux, P. Clayette, C. Kreuz, J. Chang, Y. K. Hwang, V. Marsaud, P. Bories, L. Cynober, S. Gil, G. Férey, P. Couvreur and R. Gref, *Nat. Mater*., 2010, **9**, 172.
38 N. A. Ramsahye, T. K. Trung, L. Scott, F. Nouar, T. Devic, P. Horcajada, E. Magnier, O. David, C. Serre and P. Trens, *Chem. Mater*., 2013, **25**, 479.
39 J. J. Du, Y. P. Yuan, J. X. Sun, F. M. Peng, X. Jiang, L. G. Qiu, A. J. Xie, Y. H. Shen and J. F. Zhu, J. *Hazard. Mater*., 2011, **190**, 945.
40 T. Hirakawa and Y. Nosaka, *Langmuir*, 2002, **18**, 3247.
41 G. Liu, P. Niu, L. C. Yin and H. M. Cheng, *J. Am. Chem. Soc*., 2012, **134**, 9070.
42 H. Z. Bao, X. Chen, J. Fang, Z. Q. Jiang and W. X. Huang, *Catal. Lett*., 2008, **125**, 160.